

Delineation of long-wavelength magnetic anomalies over Central India by rectangular harmonic analysis

B R ARORA and S Y WAGHMARE

Indian Institute of Geomagnetism, Colaba, Bombay 400 005, India

MS received 24 February 1984; revised 14 August 1984

Abstract. The method of rectangular harmonic analysis is applied to the geomagnetic field data from central India to isolate long wavelength magnetic anomalies associated with large-scale crustal structures. The long-wavelength anomalies have accounted for approximately 20% of the spatial variability of the residual magnetic field over the International Geomagnetic Reference Field. On the magnetic anomaly map, reflecting the surface expression of long-wavelength anomalies, the Tapi-Narmada-Son zone is characterized by a feeble positive anomaly bounded by a strong negative anomaly. The anomaly pattern is believed to be caused by the large-scale undulation in Moho and related variations in the thickness of the lower (basaltic) crust. The other two prominent anomalies, the magnetic low striking northwest and the magnetic high trending east-northeast, appear to be related to the deep structural feature of the Godavari graben and the eastern Rajasthan lineament respectively.

Keywords. Magnetic anomalies; rectangular harmonic analysis; crustal structures.

1. Introduction

Improved processing techniques of satellite magnetic data have provided new insights into the existence of magnetic anomalies with spatial wavelengths equalling the circumference of the earth down to about 250 km (Zietz *et al* 1970; Regan *et al* 1975; Langel *et al* 1982a, b). The anomalies with wavelengths shorter than 2000 km or so are believed to originate from sources in the crust or upper mantle (Bullard 1967; Hall 1974). Since the lower limit of the anomaly producing block does not exceed the depth of the Curie point isothermal surface located well within the crust, it is believed that there are probably no sources of magnetic anomaly in the mantle. The recent work of Krutikhovskaya and Pashkevich (1977, 1979), Wasilewski and Mayhew (1982), Schnetzler and Allenby (1983) point to the lower crust as a realistic source of long-wavelength anomalies. In view of the importance of these anomalies as a means of studying the large-scale crustal structure, increasing emphasis is laid on developing the analytical techniques for accurately isolating them from geomagnetic measurements, which have dominant contributions from sources in the core as well as surface geological structures, and from variations associated with currents in the ionosphere and the magnetosphere.

Spherical harmonic expansions (SHE) are often used to map the surface expressions of geomagnetic field potential. Spherical harmonic analysis (SHA) carried out to a degree and order n will resolve wavelengths, all the way, from the circumference (c) of the earth down to a wavelength of c/n (Bullard 1967). The shortest wavelength resolved through SHA being a function of n , resolution of anomalies with wavelengths of a few hundred kilometers would require SHA with very high n , *i.e.* involving an abnormally large number of coefficients, which are computationally difficult to handle even with third

generation computers. More recently, Alldredge (1981) has developed a novel method, termed rectangular harmonic analysis (RHA) wherein this limitation of SHA can be overcome by analysing the data of the residual magnetic field separately, unaccounted by SHA, from restricted areas of the globe.

The basic principle underlying the method is that not only the magnetic field potential but each of the rectangular components of the field is a solution of Laplace's equation and is, therefore, by definition, a harmonic function. In RHA, the dimension of the survey area is taken to be a fundamental wavelength, the harmonics of which permit resolution of much shorter wavelengths than are available to SHA. In regard to the definition of fundamental wavelength and exploitation of harmonic functions of shorter wavelengths, the RHA is similar in many respects to the discrete Fourier transform (DFT) approach; but one merit of the RHA method, in common with SHA, is that it derives a potential function from which one can compute all the components, and these would be consistent with the potential theory. In contrast, in DFT each element is analysed independently and thus provides no constraint to the consistency among components. RHA when coupled with SHA can be effectively used to compile the regional geomagnetic reference field. However, when analysed independently rectangular harmonic coefficients (RHC), or two-dimensional maps compiled by synthesizing the RHC, will permit identification of magnetic features originating from a particular stratum of the crust. This advantage arises from the fact that the anomaly map so compiled will be free from very long wavelength anomalies characteristic of core sources and at the same time will not include contributions from short wavelength anomalies caused by near-surface geological structures. To assess the suitability of RHA in compiling magnetic anomaly maps in the wavelength interval of 200–1400 km, an RHA is carried out on the data of geomagnetic field components obtained from a set of 1st order repeat-magnetic stations over the central part of India.

2. Tectonic features of the area of study

The rectangular area bounded by the latitudes 18°N and 30°N and longitudes 72°E and 84°E, encompassing several tectonic structures of central India, is chosen for the study. The most spectacular feature of the area is the Tapi-Narmada-Son lineament stretching from about Bombay in the west to the northeastern extremity of the sub-continent. This prominent lineament has attracted the attention of several workers and has been shown to be a major rift zone (Pascoe 1965; Biswas and Deshpande 1973; Agarwal and Gaur 1972; Roy 1971; Kailasam 1979; Mishra 1977). In contrast, Ghosh (1976) has considered the Narmada-Son lineament as representing an erosional post-Deccan trap Narmada valley formed at the crest of a domal upwarp. The lineament which denotes an effective dividing line between the Vindhyan basin to the north and Gondwanas to the south is flanked by the Vindhyan and Satpura hills on the north and south respectively. Kailasam (1979) considered these hills the uplifted shoulder of the Narmada rift zone. Based on the anomalous dependence of bouguer gravity on the elevation, Qureshi (1964, 1971) considered the Satpura and the northeast-southwest striking Aravalli mountain range as representing the horst-like structures resulting from tectonic activation of the Indian shield. The other structural features of prominence are the north-west trending Godavari valley, Bundelkhand granites and

eastern ghats. The southwest corner of the area is covered by plateau basalts of the Deccan trap.

3. Data and analysis

For compiling regional isomagnetic charts and to have a better estimate of the secular variation, the Survey of India office has laid down a set of repeat magnetic stations where geomagnetic field measurements are recorded periodically. The distribution of repeat magnetic stations in the area of study is shown in figure 1. Spot measurements of the three geomagnetic components namely declination (D) and the horizontal (H) and vertical (Z) intensities are made at each of the stations. The complete coverage of the country's repeat stations is obtained over a couple of years and the survey is repeated once in every five years. In the present analysis, observations taken over the years 1966 to 1970 are used. With the aid of the data from the permanent magnetic observatories, repeat stations data were first corrected for diurnal and disturbance effects and were then reduced to the common epoch of 1970, by applying a correction equal to the change in the field values between the date of actual observations and the fixed epoch.

The various mathematical steps involved in RHA are detailed in Alldredge (1981) and hence are not repeated here. However, to understand the significance of various terms

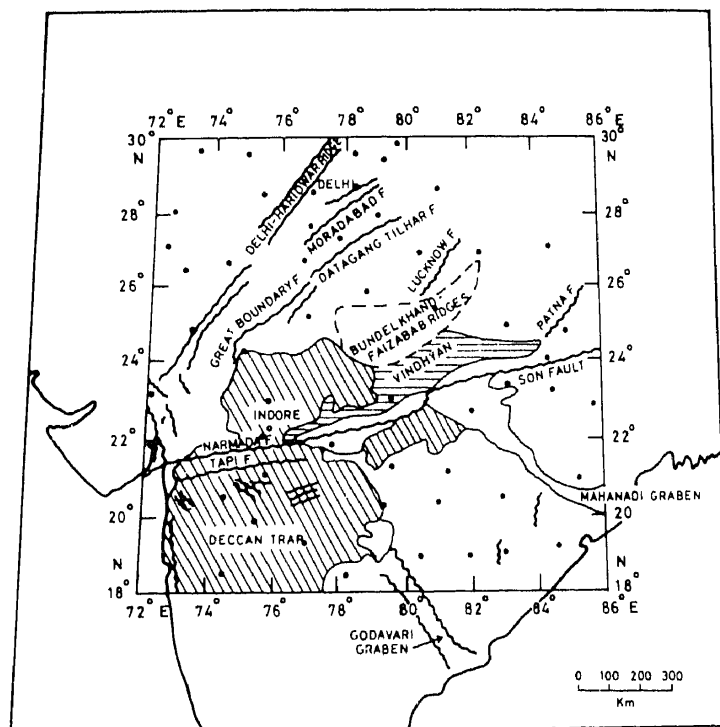


Figure 1. Map of central India showing structural trend and distribution of repeat geomagnetic stations used in rectangular harmonic analysis.

involved it should be noted that magnetic field potential is expressed in the following form:

$$\begin{aligned}
 V = Ax + By + Cz + \sum_{q=1}^{N_{\max}} \sum_{i=1}^q \left\{ D_{ij} \cos \frac{i2\pi x}{L_x} \cos \frac{j2\pi y}{L_y} \right. \\
 + E_{ij} \cos \frac{i2\pi x}{L_x} \sin \frac{j2\pi y}{L_y} + F_{ij} \sin \frac{i2\pi x}{L_x} \cos \frac{j2\pi y}{L_y} \\
 \left. + G_{ij} \sin \frac{i2\pi x}{L_x} \sin \frac{j2\pi y}{L_y} \right\} \exp \left[\left(\frac{i2\pi}{L_x} \right)^2 + \left(\frac{j2\pi}{L_y} \right)^2 \right]^{1/2} z \quad (1)
 \end{aligned}$$

where $j = q - i + 1$.

The form of the expression for each field component is obtained by taking the negative gradient of (1), e.g.

$$B_x = -\frac{\delta V}{\delta x}; \quad B_y = -\frac{\delta V}{\delta y}; \quad B_z = -\frac{\delta V}{\delta z}; \quad (2)$$

x , y and z denote the Cartesian co-ordinates of the stations with the origin at some point in the study area. L_x and L_y are the overall lengths in the direction of the x and y axes respectively. i and j are integers and N_{\max} , the maximum degree of RHA, is determined by the size of the area covered and the density of data that are available. A , B , C , D_{ij} , E_{ij} , F_{ij} and G_{ij} are the set of RHC to be evaluated.

It should also be noted that in the formulation developed by Alldredge, the input magnetic component data, B_x , B_y and B_z in (2), are the residual fields after eliminating the parts associated with the spherical harmonic model from observed data. Furthermore, residual field components are defined in the Cartesian rather than in the spherical coordinate system in which the initial measurements are reckoned. To this effect, using spherical harmonic coefficients corresponding to the IGRF model of 1970 (Hurwitz *et al* 1974), field components were computed for each station site and subtracted from the respective epoch-reduced data. The spherical residual field values (X_R , Y_R , Z_R) were then transformed into B_x , B_y and B_z in the direction of the new Cartesian coordinates with the origin at 22°N and 80°E. These data together with the positional parameters were used in the expanded form of (2) to obtain 159 observational equations, one for each component at each of the 53 stations, which in turn were used for the least square determination of the RHC. The resulting RHC are listed in table 1. In the above computation L_x and L_y were respectively taken as 1.4×10^3 km and 1.6×10^3 km, being the dimension of area along the x and y directions. N_{\max} was 5, so that the shortest wavelength resolved (L_x/N_{\max} or L_y/N_{\max}) was compatible with station spacing (approximately twice the station spacing). To test the statistical significance of RHC, the associated standard errors were evaluated and are incorporated in table 1. A coefficient is considered to be statistically significant at 95% level if its value exceeds the corresponding standard error 1.95 times. Application of this criterion suggests that many of the coefficients are not significantly determined. Root mean square (RMS) errors, derived from the differences between the input data and those calculated through RHC, are given in table 2, separately for each component. For comparison, initial RMS of input data are also included.

In order to obtain the spatial expressions of variation associated with wavelengths resolved through RHA, the magnetic field components (B_x , B_y and B_z) are computed for

Table 1. Rectangular harmonic coefficients in (1) for Central India

<i>i</i>	<i>j</i>	<i>D</i> _{<i>ij</i>}		<i>E</i> _{<i>ij</i>}		<i>F</i> _{<i>ij</i>}		<i>G</i> _{<i>ij</i>}	
		coeff	<i>S</i>	coeff	<i>S</i>	coeff	<i>S</i>	coeff	<i>S</i>
1	1	28.5	43.7	9.1	40.0	98.1	44.2	-90.5	41.0
1	2	12.9	25.7	25.7	25.4	-46.7	26.1	67.5	26.6
2	1	50.8	25.4	- 8.3	20.2	-57.8	26.9	59.9	21.1
1	3	- 8.6	15.0	-14.7	15.1	- 5.8	16.7	7.5	16.5
2	2	-35.2	18.2	18.4	18.4	35.8	18.5	-23.0	18.3
3	1	- 6.3	14.6	-24.4	13.0	- 0.02	14.7	45.8	12.6
1	4	- 2.6	9.9	5.4	9.6	- 7.8	11.6	6.4	11.3
2	3	- 2.0	13.3	-15.4	14.1	9.5	13.1	17.5	13.9
3	2	8.0	11.7	-26.6	13.1	26.1	12.0	4.9	12.4
4	1	2.6	8.9	3.7	7.9	23.3	8.9	3.9	7.9

A 24.76 19.86; B -51.25 19.72; C 112.0 21.61

Table 2. Root mean square values of the residual as well as of the input data.

	<i>B</i> _{<i>x</i>}	<i>B</i> _{<i>y</i>}	<i>B</i> _{<i>z</i>}
RMS of residual data	82.7	66.1	81.8
RMS of input values	101.0	85.3	101.4
Percentage reduction in residual data	18.93	22.50	19.23

1° × 1° grid points of the area under consideration and the contour map is drawn. Two sets of maps were prepared for each component, one employing the field values derived using all RHC and the second based on only those coefficients which were above the stipulated confidence level. Surprisingly both sets presented more or less a similar pattern suggesting that the contribution from poorly determined coefficients to the individual field values is rather insignificant. The contour maps for *B*_{*x*}, *B*_{*y*} and *B*_{*z*}, pertaining to the set using significant coefficients, are given in figures 2 a, b and c respectively.

4. Results and discussion

It follows from table 2 that the application of RHA on the residual magnetic field (*i.e.* field not accounted for by SHA) results in about 20% reduction in the RMS values indicating that the long wavelength anomalies resolved through RHA account for about 20% of the spatial variability of the residual magnetic field. The substantial magnitude of RMS even after the RHA, warrant the inference that the magnetic measurements have a substantial contribution from near surface sources.

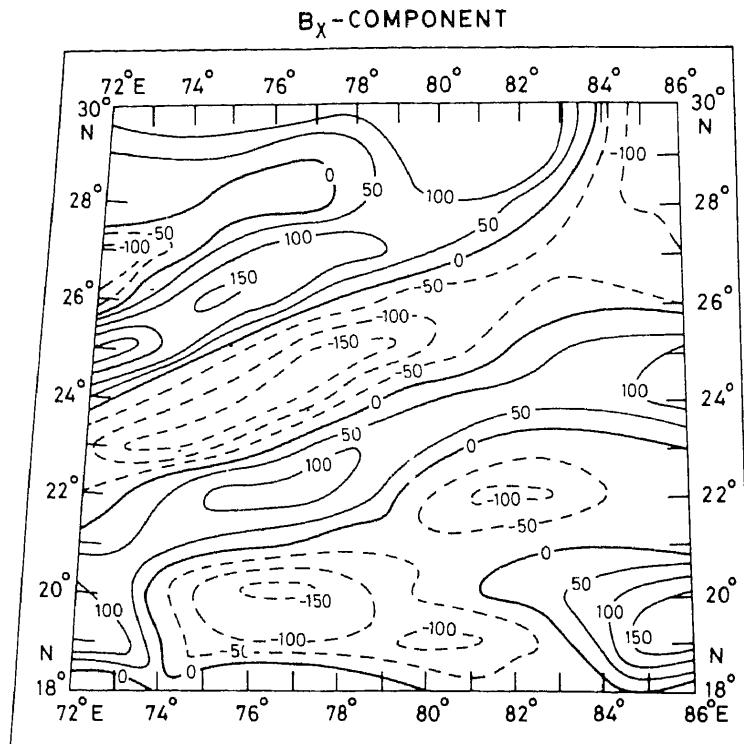


Figure 2a. Contour map showing surface expression of long-wavelength anomalies in the north-south (B_x) component of the geomagnetic field, delineated through rectangular harmonic analysis.

The anomaly patterns shown in figures 2a and c are characterized by ENE-WSW trending anomalies in the B_x and B_z components over the central part. The B_y anomalies are weak and show no pronounced pattern. On the B_z map, the most noteworthy features are the two magnetic lows striking ENE-WSW. The lows are more pronounced on the western half and are separated by a feeble positive anomaly. A more or less similar pattern with slight positional shift is noticed on the B_x component. The positive anomaly surrounded by negative anomalies stands out more prominently on the B_x map than on the B_z map. The line of zero B_x anomaly coincides with the axis of either low or high anomaly on B_z map. The positive B_x anomaly falls over the Tapi-Narmada-Son lineament and the adjoining lows encompass the Satpura mountain chain, the Vindhyan ranges and the Malwa Plateau. It is interesting that Qureshi (1982) noted a more or less similar feature on the residual isostatic gravity anomaly map of India. He found that the Tapi-Narmada-Son zone was a broad region of gravity 'high' in which Narmada-Son lineament is marked by a narrow gravity 'low'. In agreement with the hypothesis of Ghosh (1976), Qureshi interpreted the feature of gravity anomaly by considering the Tapi-Narmada-Son region as a domal upwarp with a crustal depression along the Narmada-Son lineament. A couple of deep seismic sounding profiles shot across the Narmada-Son Lineament have delineated large scale undulations in Moho. The crustal depth section along the Ujjain-Mahan profile shows a big depression in Moho, attaining a depth of about 38–40 km between Narmada and

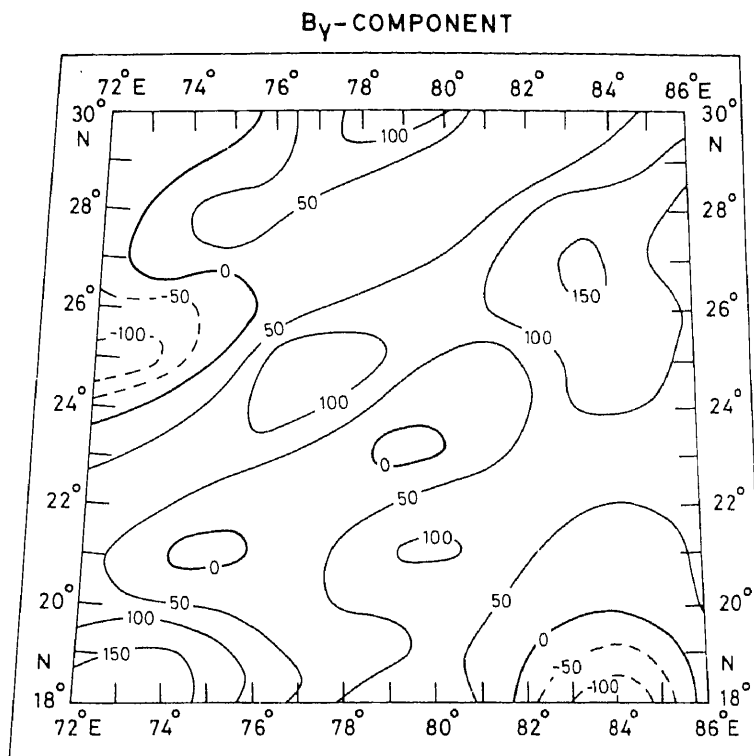


Figure 2b. Same as figure 2a but for east-west (B_y) component.

Tapi Rivers (Kaila 1984). South of the Narmada river, a large graben, termed the Tapi Graben, about 200 km in length extending in the WNW-ESE direction and about 100 km in width has been also revealed under a thin cover of Deccan Traps. The Mehmada-bad-Billimora profile in the Cambay basin indicates the Jambusar-Broach crustal block, a well-known broad regional syncline, to be a major graben (Kaila *et al* 1981). The above investigations have also revealed that the granitic basement lies at a shallow depth of about 10 km. This implies thickening of the basaltic layer under the Broach and Tapi Grabens. Towards the north and south of these grabens, the Moho as well as the granitic basement are found to be at shallower depths. Along the Mehmada-bad-Billimora profile, the rise in Moho has been shown to be more steep on the southern parts of the graben. Kaila and Krishna (1979) have inferred that the Moho have risen to quite a shallow depth, about 20 km, in the Navsari-Billimora block, beyond which the Moho may again be going deeper. As a result of this larger upwarping of Moho, crustal thickness along the Mehmada-bad-Billimora profile reduces to about 18 km under Billimora and the top of basaltic layer has been identified at a depth of 6 km. It is interesting to note that the region of larger crustal thickness, deeper Moho, in the Narmada-Son zone is characterized by positive magnetic anomalies in figures 2a and c and the areas of shallower Moho are marked by negative anomalies. This parallelism between magnetic anomaly features and the large-scale undulations in Moho is consistent with the hypotheses of Krutikhovskaya and Pashkevich (1977, 1979), Wasilewski and Mayhew (1982), Schnetzler and Allenby (1983) and several others, that

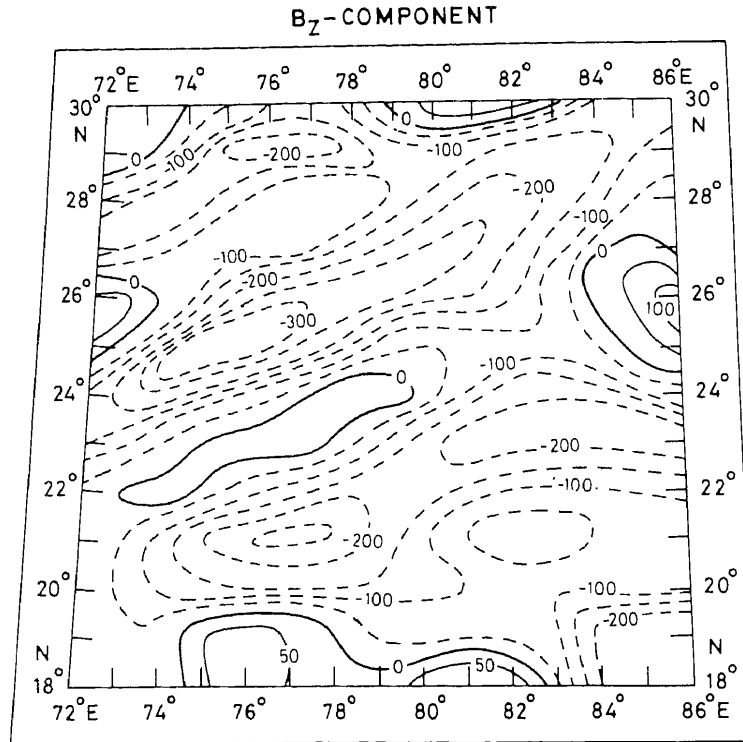


Figure 2c. Same as figure 2a but for vertical (B_z) component.

the most probable cause of long wavelength magnetic anomalies is related to the varying thickness or magnetization of the lower (basaltic) crust.

The influence of the Godavari graben on magnetic anomaly maps is marked by the presence of a magnetic low in B_x -component around 19°N, 80°E. The overall anomaly pattern is roughly aligned with the strike of the graben and appears as an extension of dominant low running ENE-WSW. The adjoining magnetic high with centre around 19°N, 85°E on the B_x map may be associated with Charnockite-Khondalite formation of Archean age. Yet another important feature is the prominent positive anomaly in the B_x component located between 24°–26°N along the 72°E longitude with a ENE-WSW trend. On the B_z component, a broad negative anomaly overlying this area becomes less pronounced along the zone of the above mentioned B_x -anomaly, giving an appearance of apparent high embodied in the regional negative trend. This anomaly pattern on the B_x and B_z components matches with the great Rajputana and Dataganj-Tilhar faults both in terms of orientation and spatial extension. The Great Rajputana fault, which separates the Vindhya on its east from the older Precambrian formations to its west, has been shown to be a deep-seated fault extending well upto the lower crust (Heron 1953). From the linear alignment of gravity anomalies and bounding linears, as indicated by the Landsat imagery, along the Great Rajputana fault, Qureshi (1982) has referred to this zone, as the eastern Rajasthan lineament.

A curious feature of the B_x -anomaly map which calls for attention is that the anomaly pattern along the 76°E longitude oscillates successively between positive and

negative values. Since, in the method adopted here, anomalies are resolved through harmonic functions, a doubt arises whether the cyclic behaviour of the anomalies is due to some computational problems. One such problem may perhaps be related to the inclusion of limited harmonic terms in the expression representing the potential field (1). However, the good correlation of anomaly patterns with the known tectonic framework and the absence of cyclic nature on the B_y and B_z maps, particularly when all components are derived from the same potential function, suggest that the noted feature is more likely to be real rather than indicating only a limitation of the analysis procedure. Nevertheless, a fresh analysis with more closely spaced data sets, thereby permitting the use of a higher degree of RHA, would provide an independent check on the results presented here as well as establish the credibility of the method. One such data set may become available soon from the reduction and analysis of the MAGSAT data.

5. Conclusions

The present analysis, though of a preliminary nature, has clearly demonstrated the utility of rectangular harmonic analysis in compiling the magnetic anomaly map corresponding to the long wavelength anomalies. The magnetic anomaly pattern over the Tapi-Narmada-Son region appears to be related to the varying thickness of the crust. The magnetic low paralleling the Godavari graben and the magnetic high along the Rajasthan lineament bring out the deep-seated nature of these structures.

Acknowledgements

The authors thank Prof B P Singh for introducing us to the problem and for illuminating discussions, and to Prof D R K Rao for his helpful comments on earlier drafts of this paper.

References

- Agarwal P N and Gaur V K 1972 *Tectonophysics* **15** 287
Alldredge L R 1981 *J. Geophys. Res.* **86** 3021
Biswas S K and Deshpande S V 1973 *J. Geol. Soc. India* **14** 134
Bullard E C 1967 *Earth Planet. Sci. Lett.* **2** 293
Ghosh D B 1976 *Geol. Surv. India. Misc. Publ.* **34** 119
Hall D H 1974 *J. Geophys.* **40** 403
Heron A M 1953 *Mem. Geol. Surv. India* **79** 37
Hurwitz L, Fabiano E B and Peddie N W 1974 *J. Geophys. Res.* **79** 1716
Kaila K L 1984 Int. Sym. Deep structure of the continental crust: Results from reflection seismology, June, Cornell Univ. New York.
Kaila K L and Krishna V G 1979 *Geophysics* **44** 1064
Kaila K L, Krishna V G and Mall D M 1981 *Tectonophysics* **76** 99
Kailasam L N 1979 *Tectonophysics* **61** 243
Krutikhovskaya Z A and Pashkevich I K 1977 *Can. J. Earth Sci.* **14** 2714
Krutikhovskaya Z A and Pashkevich I K 1979 *J. Geophys.* **46** 301
Langel R A, Phillips J D and Horner R J 1982a *Geophys. Res. Lett.* **9** 269
Langel R A, Schnetzler C C, Phillips J D and Horner R J 1982b *Geophys. Res. Lett.* **9** 273
Mishra D C 1977 *Earth Planet. Sci. Lett.* **36** 301

- Pascoe E H 1965 *A manual of the geology of India and Burma*; Manager of Publications, Govt. of India, New Delhi, Vol. I
- Qureshi M N 1964 22nd Int. Geol. Congr., New Delhi p. 490
- Qureshi M N 1971 *J. Geophys. Res.* **76** 545
- Qureshi M N 1982 *Photogrammetria* **37** 161
- Regan R D, Cain J C and Davis W M 1975 *J. Geophys. Res.* **80** 794
- Roy A K 1971 *Bull. Geol. Surv. India Ser. B* No. 30, Manager of Publications, Delhi
- Schnetzler C C and Allenby R J 1983 *Tectonophysics* **92** 33
- Wasilewski P J and Mayhew M A 1982 *Geophys. Res. Lett.* **9** 329
- Zietz I, Andreasen G E and Cain J C 1970 *J. Geophys. Res.* **75** 4007